Polar Biology
October 2010, Volume 42, Issue 10, Pages 1787-1799
https://doi.org/10.1007/s00300-019-02507-2
https://archimer.ifremer.fr/doc/00499/61066/

Decoupling light harvesting, electron transport and carbon fixation during prolonged darkness supports rapid recovery upon re-illumination in the Arctic diatom *Chaetoceros neogracilis*

Lacour Thomas [1, 2, 3, *], Morin Philippe-Israël [1, 2], Sciandra Théo [1, 2], Donaher Natalie [4], Campbell Douglas A. [4], Ferland Joannie [1, 2], Babin Marcel [1, 2]

[1] Takuvik Joint International Laboratory, CNRS (France) & ULaval (Canada), Département de BiologieUniversité LavalQuébec, Canada
[3] IFREMER, Physiol & Biotechnol Algae LabsNantes Cedex 03, France
[4] Department of BiologyMount Allison UniversitySackville, Canada

* Corresponding author : Thomas Lacour, email address : Thomas.Lacour@ifremer.fr

Abstract :

During winter in the Arctic marine ecosystem, diatoms have to survive long periods of darkness caused by low sun elevations and the presence of sea ice covered by snow. To better understand how diatoms survive in the dark, we subjected cultures of the Arctic diatom *Chaetoceros neogracilis* to a prolonged period of darkness (1 month) and to light resupply. *Chaetoceros neogracilis* was not able to grow in the dark but cell biovolume remained constant after 1 month in darkness. Rapid resumption of photosynthesis and growth recovery was also found when the cells were transferred back to light at four different light levels ranging from 5 to 154 µmol photon m−2 s−1. This demonstrates the remarkable ability of this species to re-initiate growth over a wide range of irradiances even after a prolonged period in the dark with no apparent lag period or impact on survival. Such recovery was possible because *C. neogracilis* cells preserved their Chl a content and their light absorption capabilities. Carbon fixation capacity was down-regulated (ninefold dark decrease in PCm) much more than was the photochemistry in PSII (2.3-fold dark decrease in ETRm). Rubisco content, which remained unchanged after one month in the dark, was not responsible for the decrease in PCm. The decrease in PSII activity was partially related to the induction of sustained non-photochemical quenching (NPQ) as we observed an increase in diatoxanthin content after one month in the dark.

Keywords : Arctic microalgae, Polar night, Diatom, Darkness, Photosynthesis, Growth rate, Temperature

Acknowledgment

We thank a joint contribution to the research programs of UMI Takuvik, ArcticNet (Network Centres of Excellence of Canada), the Canada Excellence Research Chair in Remote Sensing of Canada's New Arctic Frontier, and the Canada Research Chair program.

Introduction

Diatoms are ubiquitous in the surface ocean, including at very high latitudes in the Arctic where they are the most abundant microalgae in ice and in the phytoplankton community (Poulin et al. 2011). During winter, light in the surface ocean is very low due to low sun elevations and the presence of sea ice generally covered by snow (McMinn et al. 1999, Mundy et al. 2009, Leu et al. 2015). Several studies have reported on the ability of polar diatoms to survive long periods of darkness and resume fast growth as soon as light becomes available (Smayda and Mitchell-Innes 1974, Palmisano and Sullivan 1982, 1983, Peters and Thomas 1996, McMinn et al. 1999, Wulff et al. 2008, McMinn and Martin 2013, Fang and Sommer 2017). Our study provides new insights on the physiological mechanisms of dark survival and recovery.

Various strategies may allow microalgae to cope with darkness. Several microalgae taxa develop resting stages, including cysts and spores that remain viable for up to a hundred years in the case of dinoflagellates (Lundholm et al. 2011). Nutritional versatility is another strategy whereby microalgae can use both photoautotrophy and heterotrophy to obtain energy (mixotrophy). The heterotrophic capacity of polar diatoms increases as cells go into a simulated polar night (Palmisano and Sullivan 1982). Polar diatoms can assimilate amino acids and glucose both in the light and in the dark (Rivkin and Putt 1987). Some diatoms are even capable of net heterotrophic growth in the presence of glucose (White 1974). However, to our knowledge, net heterotrophic growth of a polar diatom during a prolonged period of darkness has not been observed and the addition of organic substrates does not appear to aid their dark survival capabilities (Dehning and Tilzer 1989, Popels and Hutchins 2002).

Our current knowledge of the physiology of dark survival derives mostly from studies using non-Arctic diatoms, or from other algal groups. For instance, green algae seem to partially dismantle their photosynthetic apparatus during long periods in the dark but keep it loosely assembled to rapidly resume photosynthesis when exposed to light (Baldisserotto et al. 2005, Morgan-Kiss et al. 2006, Ferroni et al. 2007, Nymark et al. 2013). In natural communities, photosynthetic performance falls to minimal levels after several weeks of darkness (Reeves et al. 2011, Martin et al. 2012) while generally going back to a normal state nearly immediately upon the return of light (Kvernvik et al. 2018). In diatoms, dark survival is also characterized by low metabolic rates and the consumption of energy reserves (Peters 1996, Peters and Thomas 1996, Schaub et al. 2017). Diatoms can store

large quantities of lipids to buffer energy shortage (Smith and Morris 1980, Palmisano and Sullivan 1982), so a balance between energy storage and the rate of utilization may be tuned to increase survival during long periods of darkness.

In the Arctic marine environment, changes in snow optical properties was shown to be the primary driver for allowing sufficient light to penetrate through the thick snow and initiate algae growth below the sea ice (Hancke et al. 2018). Light increase can also be abrupt because of sea ice breakup and can take place at different moments of the spring and summer. Polar diatoms must thus cope with long period in darkness (or very low irradiance) and sudden light bursts of unpredictably variable intensity even after prolonged darkness. The physiological basis of such flexibility is mostly unknown. Several recent studies have examined the physiological response of polar microalgae to changes in growth irradiance (Kropuenske et al. 2009, Arrigo et al. 2010, Kropuenske et al. 2010, Mills et al. 2010, Petrou et al. 2010, Petrou et al. 2011, Petrou and Ralph 2011, van de Poll et al. 2011, Lacour et al. 2018). These studies highlighted how non-photochemical quenching (NPQ) is a crucial physiological mechanism for the survival of polar diatoms at low temperature coupled with other stresses such as high light (including UV radiations) (Petrou et al. 2016). Lacour et al. (2018) have shown, in the Arctic diatom *Thalassiosira gravida* acclimated to high irradiance, a strong sustained (hour kinetics relaxation) non photochemical quenching (NPQs). NPQ (and possibly NPQs) may play an important role to prime diatoms for sudden transitions from dark to (variable) light exposure. The purpose of this study was to describe the physiological strategy that allows polar diatoms to survive in the dark while remaining prepared for light return.

We first studied the growth and photophysiology at four different growth irradiances of *Chaetoceros. neogracilis*, one of the dominant diatoms in the Beaufort Sea (Balzano et al. 2012, Balzano et al. 2017) after one month in darkness. To understand how *C. neogracilis* manage such recovery, we described in detail the physiological state of the cells after one month in the dark from light capture to carbon fixation.

Material and methods

Algal Cultures

We performed two independent experiments: a light recovery experiment (Exp 1) and a dark acclimation experiment (Exp 2). In Exp 1, unialgal cultures of *C. neogracilis* (Roscoff Culture Collection RCC 2278), isolated during the Malina cruise (2009) in the Beaufort sea (Balzano et al. 2012) were grown in semi-continuous cultures of 2000 mL in pre-filtered f/2 medium (Guillard 1975) enriched with silicate. Salinity was 35 PSU. The illumination was provided continuously by white fluorescent tubes at 23 µmol photon m^{-2} s^{-1} as measured using a QSL-100 quantum sensor (Biospherical Instruments, San Diego, CA, USA) placed in the culture vessel. Culture conditions were maintained semi-continuously by diluting cultures once a day in order to maintain biomass semi-constant (MacIntyre and Cullen 2005) and gently aerated through 0.3 µm-pore-filters. Cultures were grown in a growth chamber (Percival Scientific Inc., Perry, IA, USA) that allowed temperature maintenance at 0°C (± 1°C). Triplicate cultures were then incubated in complete darkness for 30 days and then illuminated by white fluorescent tubes (Phillips®, 54W/840) at 4 different light levels (L/D, 12h/12h) with mean daily irradiances of 5, 27, 41, and 154 µmol photon m^{-2} s^{-1} (± 5%) and maximum irradiances (at noon) of 531, 141, 93 and 17 µmol photon m^{-2} s^{-1} (see Online resource 1) controlled by a specific sofware (IntellusUltraConnect, Percival Scientific Inc., Perry, IA, USA). Those irradiances roughly correspond to the mean daily irradiances encountered between 70 and 80°N in March, April, May and June respectively (seasonal change in day length was not mimicked due to technical considerations). We monitored cell number and photochemical characteristics over 8 to 14 days following re-illumination (Experiment 1: light recovery). Triplicate culture were sampled at the first sunrise (t0) and several time during the first light period. Then, the cultures were sampled each day at noon.

In Exp 2, triplicate cultures were also acclimated to 23 µmol photon m^{-2} s^{-1} (continuous light) or to complete darkness for 30 days before sampling for comparisons of cell number, pigments, particulate carbon and nitrogen, carbon fixation, Photosystem II (PSII) photochemical activity and Rubisco content (RbcL) (Experiment 2: dark acclimation).

Cell number, C and N, pigments

Chaetoceros neogracilis cells were counted and sized (equivalent spherical diameter) before and after culture dilution using a Beckman Multisizer 4 Coulter Counter. The concentrations of particulate C and N were determined daily on triplicate samples. For particulate carbon and nitrogen, an aliquot of 10 mL of algal culture was filtered onto glass-fiber filters (0.7 µm, 25 mm) pre-combusted at 500°C for 12 h. Filters were kept desiccated before elemental analysis with a CHN analyzer (2400 Series II CHNS⁄O; Perkin Elmer, Norwalk, CT, USA). For pigment analysis, an aliquot of algal culture (5 mL) was filtered onto a GF/F glass-fiber filter, immediately flash-frozen in liquid nitrogen and stored at -80°C until analysis by HPLC using the protocol described in Zapata et al. (2000). Sample filtration were done as fast as possible (< 2 min) under very low green light. The xanthophyll de-epoxidation state (DES in %) was calculated as Dt/(Dd + Dt)*100, where Dd is the concentration of Diadinoxanthin, the epoxidized form and Dt is that of Diatoxanthin, the de-epoxidized form (Lavaud et al. 2007).

Carbon fixation

The relationship between the rate of carbon fixation (P) and irradiance (E) (P vs E curve) was determined according to Lewis and Smith (1983). A 50-mL sample was collected in each replicate culture, and inoculated with inorganic ^{14}C ($NaH^{14}CO_3$, 2 µCi mL^{-1}). To determine the total amount of bicarbonate added, three 20-µL aliquots of inoculated culture sample were added to 50 µL of an organic base (ethanolamine) and 6 ml of the scintillation cocktail (Ecolume) into glass scintillation vials. Then 1-mL aliquots of the inoculated culture sample were dispensed into twenty-eight 7-mL glass scintillation vials already cooled in their separate thermo-regulated cavities (0 or 5°C). The vials were exposed to 28 different light levels provided by independent LEDs (LUXEON Rebel, Philips lumileds) from the bottom of each vial. The PAR (µmol photon m^{-2} s^{-1}) in each cavity was measured before incubation with an irradiance meter (Biospherical QSL-100) equipped with a 4π spherical quantum sensor. After 20 minutes of incubation, culture aliquots were fixed with 50 µL of buffered formalin then acidified (250 µL of HCl 50%) under the fume hood for 3 hours in order to remove the excess inorganic carbon (JGOFS protocol, UNESCO 1994). Finally, 6 mL of scintillation cocktail were added to each vial prior to counting in the liquid scintillation counter (Tri-Card, PerkinElmer). The chlorophyll-specific carbon fixation rate was finally computed according to Parsons et al. (1984).

Fluorescence measurements

Photochemical properties of PSII were determined by variable fluorescence using a Fluorescence Induction and Relaxation (FIRe) fluorometer (Satlantic, Halifax, NS, Canada) that applies a saturating, single turnover flash (STF, 100µs) of blue light (455 nm, 60-nm bandwidth) to the incubated sample to generate a fluorescence induction curve (detected at 680 nm) that can be used to estimate the minimum fluorescence (F_0 for dark-adapted and F_S for light-adapted samples), the maximum fluorescence (F_m if dark-adapted and F_m' if light-adapted) and the effective absorption cross section of PSII (σ_{PSII} if dark-adapted and σ'_{PSII} if light-adapted) using the FIReWORX algorithm (Pers. Comm. Audrey Barnett, www.sourceforge.net) and the flash lamp calibration provided by the instrument manufacturer (Thomas and Campbell 2013). We found that 20 min in darkness was sufficient to fully relax non-photochemical quenching of F_0 and F_m. F_s, F_m' and σ'_{PSII} were measured repeatedly on the same culture subsample after 2 min exposures under an increasing range of actinic light levels.

We estimated the maximum quantum yield of PSII (F_v/F_m) and the optical absorption cross section (σ^{OPT}_{PSII}) from 20 min dark acclimated cells (Huot and Babin 2010) and the realized quantum yield of charge separation at the PSII (Φ_{PSII}, Genty et al. (1989)) as:

$$F_v/F_m = \frac{F_m - F_0}{F_m} \qquad \textbf{Equation 1}$$

$$\sigma^{OPT}_{PSII} = \frac{\boldsymbol{\sigma_{PSII}}}{\mathbf{F_v/F_m}} \qquad \textbf{Equation 2}$$

$$\Phi_{PSII} = \frac{F_m' - F_s}{F_m'} \qquad \textbf{Equation 3}$$

To quantify the partitioning of excitation energy between photochemistry, fluorescence and thermal dissipation, we used the approach of Hendrickson et al. (2004). Φ_{PSII} corresponds to the fraction of absorbed irradiance used for photochemistry, $\Phi_{f,D}$ is the sum of the fractions that are

lost by either thermal dissipation or fluorescence and Φ_{NPQ} is the fraction that is thermally dissipated via ΔpH and/or xanthophyll-regulated processes:

$$\Phi_{f,D} = \frac{F_s}{F_m} \quad \textbf{Equation 4}$$

and

$$\Phi_{NPQ} = \frac{F_s}{F_{m'}} - \frac{F_s}{F_m} \quad \textbf{Equation 5}$$

The PSII specific electron transport rate (ETR, e^- $PSII^{-1}$ s^{-1}) was calculated as (Suggett et al. 2010):

$$ETR = \sigma_{PSII} \cdot \frac{\Phi_{PSII}}{F_v/F_m} \cdot E \cdot 6.022\ 10^{-3} \quad \textbf{Equation 6}$$

where E is the actinic irradiance (µmol photon m^{-2} s^{-1}), σ_{PSII} is the effective absorption cross-section of PSII (A^2 $PSII^{-1}$) measured from dark acclimated samples and 6.022 10^{-3} is a constant to convert σ_{PSII} to m^2 µmol $photon^{-1}$.

A proxy for the amount of active PSII was estimated as (Oxborough et al. 2012, Silsbe et al. 2015, Murphy et al. 2017):

$$\text{PSII chl a}^{-1} \sim k \times \frac{F_O}{\sigma_{PSII} \times [\text{Chl a}]} \quad \textbf{Equation 7}$$

where k is an unknown constant.

Data analysis. The initial slope (α, g C g^{-1} Chl *a* h^{-1} (µmol photon m^{-2} s^{-1})$^{-1}$ and α^{ETR}, e^- $PSII^{-1}$ (µmol photon m^{-2})$^{-1}$) and the maximum value of the rate versus E curves (P_m, d^{-1} and ETR_m e^- $PSII^{-1}$ s^{-1}) were estimated by fitting the equation of Platt et al. (1980) (with the photoinhibition parameter β) to the experimental rate and PAR values as:

$$P = P_m\,(1 - e^{-\frac{\alpha E}{P_m}})e^{-\frac{\beta E}{P_m}} \quad \textbf{Equation 8}$$

$$ETR = ETR_m\,(1 - e^{-\frac{\alpha^{ETR} E}{ETR_m}})e^{-\frac{\beta^{ETR} E}{ETR_m}} \quad \textbf{Equation 9}$$

The light-saturation parameters for carbon fixation (E_K, µmol photon m^{-2} s^{-1}) and for electron production at PSII (E_K^{ETR}, µmol photon m^{-2} s^{-1}) were obtained as:

$$E_K = \frac{P_m}{\alpha} \quad \textbf{Equation 10}$$

$$E_K^{ETR} = \frac{ETR_m}{\alpha^{ETR}} \quad \textbf{Equation 11}$$

Protein analyses

For RbcL quantitation, 30 mL of each culture was harvested onto GF/F filters (0.7 µm pore size, Whatman). Filters were flash-frozen in liquid nitrogen and stored at -80°C. Protein extractions were performed using the FastPrep-24 and bead lysing "matrix D" (MP Biomedicals), using 4 cycles of 60 s at 6.5 m/s in 750 µL of 1X extraction buffer (Agrisera, AS08 300). The supernatant was assayed using a detergent compatible (DC) assay kit against BGG standard (Biorad), then equalized volumes containing 0.25 µg of denatured total protein containing 1x sample buffer (Invitrogen) and 50 mM DTT were loaded onto a 4-12% Bis Tris SDS-PAGE gel (Invitrogen). Each gel was also loaded with a 5-point quantitation curve using RbcL molar standard (www.agrisera.se, AS01 017S).

Proteins were separated via electrophoresis at 200 V then transferred to polyvinylidene difluoride (PVDF) membranes at 30 V. Membranes were blocked for 1 h in 2% $_{w/v}$ ECL blocking agent (GE Healthcare) dissolved in TBS-T (Tris, 20 mM; NaCl, 137 mM; Tween-20, 0.1%$_{v/v}$), then incubated in 1:20,000 rabbit polyclonal anti-RbcL antibody for 1 h (Agrisera, AS03 037) and finally in 1:20,000 goat anti-rabbit IgG HRP conjugated antibody (Agrisera, AS10 668) for 1 h. Membranes were rinsed with TBS-T solution five times after each antibody incubation. Chemiluminscent images were obtained using ECL Ultra reagent (Lumigen, TMA-100) and a VersaDoc CCD imager (Bio-Rad). Band densities for samples were determined against the standard curve using the ImageLab software (v 4.0, Biorad).

Apparent Rubisco catalytic turnover rate (C RbcL^{-1} s^{-1}) was computed as Wu et al. (2014):

$$\text{RUBISCO catalytic turnover rate} = k^{C}_{CAT} = \frac{P^{C}_{m}}{\text{RbcL C}^{-1}} \qquad \textbf{Equation 12}$$

where P^{C}_{m} is the carbon-specific maximum fixation rate (mol C g C^{-1} s^{-1}) and RbcL C^{-1} (mol RbcL g C^{-1}) was estimated from immunoquantitation data normalized to carbon.

Light absorption

A dual beam spectrophotometer (Perkin Elmer, Lambda 850) equipped with an integrating sphere was used to determine the spectral values of the optical density (OD (λ)) of the cultures. Filtered culture medium was used as reference. The chlorophyll *a*-specific absorption coefficient (a* (λ) in m^2 mg Chla^{-1}) was calculated as follow:

$$a^*(\lambda) = \frac{2.3 \cdot OD(\lambda)}{l \cdot [Chla]} \qquad \textbf{Equation 13}$$

where l is the path length of the cuvette (0.01 m) and [Chl$a$] the chlorophyll *a* concentration (mg m^{-3}).

Statistical tests

To test for differences between light and dark with regard to physiological characteristics we used t-test. Normality was tested by a Shapiro-Wilk test. To test differences between mean growth rates in Experiment 1 performed an ANOVA. Data analyses were performed using the Sigma Plot 12.5. In the figures, asterisks indicate significant differences (one asterisk : $P<0.05$, two: $P<0.001$) between light and dark acclimated cells. In the results section, statistics are described in detail (t, F df, P). Results of Figure 5 statistics are presented in Online resource 5.

Results

Experiment 1: From darkness to light. We monitored the growth and photochemistry of cultures incubated 1 month in the dark and then exposed to 4 different light cycles (different light level but same duration of the photoperiod, see Online resource 1 and Material and methods section,). The light cycles roughly mimicked a natural light cycle and allowed a progressive increase in growth irradiance during the first hours after re-illumination. Cells were able to restart growth during the first day after light recovery (Figure 1). At day 7 and later, growth rates began to decrease due to unknown limitations in the 3 highest of the 4 light conditions. We computed the mean growth rates between days 1 and 6 (i.e when growth was not yet limited). The mean growth rates increased with mean growth irradiance between 5 and 41 µmol photon m^{-2} s^{-1} and then remained constant under higher irradiance (Anova test, $F_3=134.954$, $P<0.001$ and see the Pairwise multiple comparison procedure with Holm-Sidak method in Online resource 5). The irradiance-saturated growth rate

291 (0.43 ± 0.02 d^{-1} at 41 and 154 µmol photon m^{-2} s^{-1}) is in the range of light saturated growth rates
292 found in polar species grown at 0°C (Sakshaug 2004, Lacour et al. 2017), and slightly lower than
293 *C. neogracilis* growth rates measured under continuous illumination in semi-continuous culture
294 (0.6 d^{-1}, unpublished results). Culture growth rates did not seem affected by the dark period after
295 illumination was resumed (Figure 1B). Between 0 and 8 hours, the instantaneous growth rate
296 remained almost null in all the treatments. Growth restarted between 8 and 32 hours after re-
297 illumination at high rate (0.58 ± 0.03 d^{-1}) and was not affected by growth irradiance at this early
298 stage. After 32 hours, the instantaneous growth rates were similar to the irradiance-specific mean
299 growth rates.
300
301 The maximum PSII electron transport rate (ETR_m) increased during the first hour after re-
302 illumination in all the conditions (Figure 2A, 3A). This increase was even more pronounced at high
303 irradiance with no apparent damage to PSII even at the highest re-illumination irradiances. The
304 light saturation parameter for photochemistry (E_K^{ETR}) also increased after re-illumination,
305 apparently to acclimate to the new growth conditions (Figure 2B, 3B). The increases were
306 particularly high at high irradiance, with a 75 % increase in ETR_m and a 124% increase in E_K at
307 154 µmol photon m^{-2} s^{-1} during the first hours of exposure to light. The slope of the ETR versus E
308 curves (α^{ETR}) decreased during the first day after re-illumination and then increased and stabilised
309 at a value that was dependent on growth irradiance (Figure 2C, 3C). Our results suggest that after
310 2-3 days, cells were nearly acclimated to growth conditions as photochemical parameters (α^{ETR},
311 ETR_m and E_K^{ETR}) stabilized. Mean α^{ETR} values (measured between day 3 and 5) decreased with
312 growth irradiance (Figure 2C, D) and mean ETR_m and E_K^{ETR} increased with growth irradiance
313 (Figure 2A, B, D).
314
315 **Experiment 2: Prolonged darkness.** We compared the physiological characteristics of cells
316 acclimated to 23 µmol photon m^{-2} s^{-1} with cells incubated 1 month in complete darkness.
317 Microscopic observations did not reveal the presence of resting spores. Cells incubated in darkness
318 had a lower cell size (Figure 4A, Paired t test, $t_4 = 19.822$, $p < 0.0001$). A fraction of the cells
319 divided once during the first hours of the dark period, which may explain the decrease in the mean
320 cell size. Indeed, the total biovolume of the culture (cell volume x cell number) remained constant
321 throughout the dark period (data not shown). Cell viability was not directly assayed in this study,

so that the proportion of the cells that remained viable at the end of the dark period is unknown. However, the rapid and intense growth after light recovery suggests that most of the cells remained viable.

We observed slightly higher Chl *a* to C ratio in cells incubated in the dark (Figure 4C, Paired t test, t_4 = -2.987, p=0.04) and relatively unchanged chlorophyll specific absorption coefficient (a*, Online resource 2, Paired t test, t_{10} = 0.893, p=0.393) and optical absorption cross section of PSII (σ^{OPT}_{PSII}, Online resource 3). Cells thus maintained their ability to capture light throughout the dark period. Pigment contents remained unchanged after the dark period with the exception of xanthophylls (Figure 4D). Total xanthophyll was not changed (Paired t test, t_4 = -1.386, p =0.238) but the de-epoxidation ratio was dramatically higher in cells incubated in darkness (DES = 58, Paired t test, t_4 = -160.045, p < 0.0001). This DES was indeed higher than the DES measured in a previous study on *C. neogracilis* acclimated to very high irradiance (continuous light, 400 µmol photon m^{-2} s^{-1}; DES=27). This is an unexpected result because diatoxanthin is generally produced at high irradiances (see discussion). The C/N ratio was lower in cells incubated in the dark (Figure 4B, Paired t test, t_4 = 2.810, p =0.048). The Rubisco to carbon ratio was not significantly different between light and dark (Figure 4E, Paired t test, t_3 = -0.218, p=0.841). Unchanged Rubisco content and decreased photosynthetic capacity (see below) led to a decrease of the apparent catalytic turnover rate of Rubisco (k^C_{cat}, C s^{-1} per site) in darkness.

We used incubations at various irradiances to investigate the potential for photochemistry in cells acclimated to the light and to the dark. We used the approach of Hendrickson et al. (2004) to compare the potential fate of absorbed light energy (Figure 5 and materials and methods section). The fraction of absorbed irradiance consumed via photochemistry (Φ_{PSII}) was higher in cells acclimated to 23 µmol photon m^{-2} s^{-1} across all the incubation irradiances tested (see the results of the statistical tests in Online resource 5). The regulated thermal dissipation (Φ_{NPQ}) was also generally significantly greater in the light than in the dark (see Online resource 5). On the contrary, cells incubated 1 month in the dark showed a much larger fraction of absorbed energy consumed by non-regulated thermal dissipation and fluorescence ($\Phi_{f,D}$). $\Phi_{f,D}$ is largely dominated by thermal dissipation since fluorescence accounts for only a small fraction of absorbed excitation (Hendrickson et al. 2004). The high de-epoxidation ratio found in the dark may be responsible for

a constitutive NPQ that is measured as non-regulated thermal dissipation since short-term changes in light intensity do not alter its efficiency.

Cells incubated in the dark showed significantly lower F_v/F_m (Paired t test, $t_3 = 27.626$, $p = 0.0001$), σ_{PSII} (Paired t test, $t_3 = 14.017$, $p = 0.0007$) and $F_0/(\sigma_{PSII}$ Chl *a*) (Paired t test, $t_3 = 18.002$, $p = 0.0004$), a proxy for the content of active PSII (Figure 6A) (Oxborough et al. 2012, Silsbe et al. 2015, Murphy et al. 2017). The PSII ETR versus incubation irradiance curves were highly affected by the dark period (Figure 6B, 6C and **Online resource** 4). ETR_m and α^{ETR} were both 2.3 fold lower after 1 month in the dark, (Paired t test, $t_{10} = 9.320$, $p < 0.0001$ and Paired t test, $t_{10} = 10.336$, $p < 0.0001$ respectively), resulting in an unchanged E_K^{ETR} (Paired t test, $t_{10} = -0.411$, $p = 0.690$).

We obtained carbon fixation rate versus incubation irradiance curves (P vs E curves) for cells incubated 1 month in the dark. We compared the photosynthetic characteristics of cells incubated in the dark with cells acclimated to 3 other continuous growth irradiances (10, 50, 80 µmol photon m^{-2} s^{-1}) (see methods, Figure 7). The carbon-specific maximum fixation rate (P^C_m) was not affected by growth irradiance (Figure 7A) and was ~9 times higher than the P^C_m of cells incubated in the dark for 1 month (Figure 7B, Paired t test, $t_{10} = 31.516$, $p < 0.0001$). The Chl *a* specific initial slope of the PI curve (α^*) was also ~7 times higher in the light than in the dark (Figure 7C, Paired t test, $t_{10} = 3.998$, $p = 0.0025$). The capacity of cells incubated in the dark to fix carbon was thus initially restricted upon re-exposure to both low and high irradiance.

Discussion

Physiology of recovery. The duration of the total darkness is often longer than one month in the Arctic environment. However, most of the physiological acclimatory changes have been shown to occur during the first days of the dark period and cell physiology after one month seems to be therefore representative of the dark acclimation state (Peters and Thomas 1996). Diatoms,particularly polar species are known for their dark survival capabilities (Antia and Cheng 1970, Bunt and Lee 1972, Smayda and Mitchell-Innes 1974, Palmisano and Sullivan 1982, 1983, Murphy and Cowles 1997, Fang and Sommer 2017, Kvernvik et al. 2018). However, how they achieve survival and deal with the return to light is unclear.

In order to study light recovery from darkness in *C. neogracilis*, we used a range of light from 5 to 154 µmol photon^{-1} m^{-2} s^{-1}. We did not observe any time delay before growth resumed in any of the light regimes (Figure 1). Such rapid recovery is not a ubiquitous response in microalgae. For example, the pelagophyte *Aureococcus anophagefferens* needs more than 20 days to restart growth after 30 days in the dark (Popels and Hutchins 2002). The duration of the lag phase was shown to depend on temperature, on the duration of the dark period and on the growth phase before the dark period and may result from having a significant proportion of the cells being dead (Peters 1996, Peters and Thomas 1996, Popels and Hutchins 2002). In the field, Berge et al. (2015) showed that in Kongsfjorden (Svalbard) during the polar night, primary producers were physiologically active and able to rapidly restart photosynthesis as soon as irradiance reached 0.5 µmol photons m^{-2} s^{-1}. Our results demonstrate the strong ability of *C. neogracilis* to survive long periods of darkness and a high level of physiological plasticity allowing fast growth recovery upon re-illumination.

Our results show that the light intensity experienced during re-illumination only slightly influence the growth rate recovery. The initial growth recovery was fast and intense, as instantaneous growth rate was 0.58 d^{-1} between 8 and 32 hours, which corresponds to almost 1 doubling per day. Such a growth rate is similar to the growth rates measured in healthy light-saturated cultures of *C. neogracilis* at 0°C (unpublished results) and higher than the mean growth rate of polar species at 0°C (0.46 ± 0.23 d^{-1}, (Lacour et al. 2017)). It also indicates that most of the cells remained viable throughout the dark period. Moreover, the resumption of growth between 8 and 32 hours was also high under re-illumination with only 5 µmol photon m^{-2} s^{-1}, which is a light-limiting level for longer term growth. This suggests that the growth resumption was not fuelled mainly by photosynthesis but likely by carbon reserves. During the following days, growth stabilized at different rates, which were indeed dependent on light intensity. Such rapid recovery relies largely on the rapid acclimation of its photophysiology. The photochemical properties of the cells rapidly acclimated to the new growth conditions (Figure 2, Figure 3). Kvernvik et al. (2018) also showed rapid increases in the efficiency of photosynthetic electron transport of natural phytoplankton communities upon re-illumination. The immediate and intense increase (within 1 hour) of E_K and ETR_m suggests a re-organisation of the existing photosystems rather than *de novo* synthesis of new proteins and pigments (Peters and Thomas 1996, Baldisserotto et al. 2005, Morgan-Kiss et al. 2006, Ferroni et al. 2007, Nymark et al. 2013). It can be explained by light-induced reactivation of

enzymes involved in downstream reactions (Maxwell and Johnson 2000). The relaxation of xanthophyll-related NPQ may also account for such rapid recovery of photochemical capacity. Culture growth rates (computed between days 1 and 6) and photophysiological properties (Figure 2D) are comparable to those of this microalgae (unpublished results) and other polar microalgae cultured without previous period of darkness under comparable light intensities (reviewed in Lacour et al. (2017)).. It suggests that prolonged darkness has no impact on Arctic diatom ability to acclimate to new growth conditions.

Dark physiology. How does *C. neogracilis* prepare for rapid growth recovery?

C. neogracilis cells kept in darkness maintain their capacity to capture light, as shown by the photosynthetic pigments (Figure 4C), the chlorophyll specific absorption coefficient (Online resource 2) and the optical absorption cross section of PSII (σ^{OPT}_{PSII}, Online resource 3) that remained relatively unchanged after one month in the dark, with a*(455nm) and σ^{OPT}_{PSII} (455nm) are ≈ 0.9X of the levels found in cells acclimated to the light (data not shown). At 12°C, Chl *a* per Cell in *Thalassiosira weissflogii* was previously shown to remain constant during 2 months in total darkness (Murphy and Cowles 1997). The benefit to maintaining their light harvesting capacity is probably the ability to resume growth relatively promptly when conditions become favorable uppon re-illumination.

The potential for photochemistry was, however, drastically reduced. We observed decreases in F_v/F_m, σ_{PSII} (the effective, rather than the optical, absorption cross section) and consequently in both the light-limited (α_{ETR}) and light-saturated (ETR_m) activity of PSII. Decreases in the potential for photochemistry were observed in polar diatoms (Wulff et al. 2008, Reeves et al. 2011, Martin et al. 2012) and polar rhodophytes (Lüder et al. 2002) incubated in darkness and were interpreted as a progressive degradation of light-harvesting antennae and/or reaction centres. Nymark et al. (2013) suggested instead that decreases in α_{ETR} were explained by lower resonance energy transfer efficiency from the light-harvesting antenna pigments to the PSII reaction centre, probably resulting from structural changes within the light-harvesting antenna complexes. Our results suggest that in the case of *C. neogracilis*, the decrease of the potential for photochemistry is a regulated response to prolonged darkness rather than actual PSII damage or dismantlement. Indeed,

this decrease may be at least partially due to an accumulation of Diatoxanthin (35 fold DES increase) that induces sustained heat dissipation and thereby lowers σ_{PSII} even though pigment content and σ^{OPT}_{PSII} are maintained. Some observations in the field (Brunet et al. 2006, Brunet et al. 2007) and in culture (Deventer and Heckman 1996, Jakob et al. 1999, Lavaud et al. 2002) showed that microalgae exposed to darkness exhibit significant levels of chlororespiration. Chlororespiratory energization of the thylakoid membrane maintains a proton gradient, an activated xanthophyll cycle and an ATP synthase in an active state during dark periods, which could be advantageous upon re-exposure to light (Goss and Jakob 2010). This respiratory pathway may also provide energy to sustain metabolic activity and/or balance the ATP:reductant levels in the chloroplast under prolonged darkness. The accumulation of Dt probably keeps *C. neogracilis* cells in a photo-protected, highly dissipative state with a low conversion efficiency of absorbed light into photochemistry and thus a low risk of reactive oxygen dependent damage (Oguchi et al. 2011, Murphy et al. 2017). When light returns, *C. neogracilis* can relax xanthophyll-related NPQ to optimize light harvesting.

The potential for carbon fixation was particularly affected by darkness. Both the light-limited (α) and the light-saturated carbon-specific fixation rates (P^C_m) (20 min incubations at various irradiances) were drastically lowered in dark conditions, to an even greater degree than the drop in ETR_m. Several authors noticed a drop in photosynthetic capacity after several days in darkness (Palmisano and Sullivan 1982, Dehning and Tilzer 1989, Peters and Thomas 1996). Interestingly, the Rubisco protein content was not significantly affected by darkness. Thus, Rubisco protein pool size (Young et al. 2015) is not in this case responsible for the observed decrease in P^C_m as illustrated by the reduced apparent catalytic turnover rate of Rubisco in darkness. However, a regulated decrease in Rubisco activity could account for the decline in P^C_m. In fact, MacIntyre et al. (1997) showed thatdeactivation of the carbon assimilating machinery (e.g., RuBisCO) occur very rapidly in light–dark transitions in the chlorophyte *Dunaliella tertiolecta* and especially in the diatom *Thalassiosira pseudonana* (timescale: minute). The maintenance of the Rubisco pool size probably contributes to the rapid recovery through re-activation when light returns.

The discrepancy between the 2.3 fold dark decrease in ETR_m versus the 9 fold dark decrease of P^C_m shows that during prolonged darkness carbon fixation potential is down regulated more than

photochemistry potential per PSII. We used a proxy of the amount of active PSII per Chl *a* (Oxborough et al. 2012, Silsbe et al. 2015, Murphy et al. 2016) to understand if the number of active PSII can help to reconcile carbon fixation and photochemistry. The number of active PSII indeed decreased significantly by 1.5 fold in the dark but cannot fully account for the discrepancy between a predicted 2.3 x 1.5 = 3.5 fold decrease in the potential for electron transport and the 9 fold decrease in the potential for carbon fixation. This suggests that electrons produced at PSII are diverted away from carbon fixation when cells acclimated to prolonged darkness are re-illuminated. Schuback et al. (2017) had similar observations in Arctic field populations, particularly in assemblages exposed to short-term super-saturating irradiances. They also suggested that it could be related to an up-regulation of alternative electron pathways. Laboratory (Wagner et al. 2006, Bailey et al. 2008, Cardol et al. 2008) and field studies (Mackey et al. 2008, Grossman et al. 2010, Schuback et al. 2015, Schuback et al. 2017, Zhu et al. 2017, Hughes et al. 2018b) have examined the processes that uncouple rates of CO_2 assimilation and photosynthetic electron transport. Those pathways are generally active under high irradiance or under severe nutrient limitation, when cells are subjected to metabolic unbalance (see also the review by Hughes et al. (2018a)). After one month under complete darkness, some downstream photosynthetic processes are probably constrained, generating such metabolic unbalance. Alternative electron pathways may create an electron valve on the acceptor side of PSII and thus protect the system from photodamage by lowering the redox pressure until carbon assimilation can be re-activated. Again, upon light recovery, those alternative electron flows can be rapidly redirected to carbon fixation in order to fuel growth.

Conclusion

Polar microalgae live under extreme environmental conditions: permanently low temperatures, extreme variations in irradiance and above all, long period of complete darkness. The ability to survive such periods of darkness and to re-initiate growth when light returns affects the fitness of a phytoplankton species in this environment. This study illustrates how the Arctic diatom *C. neogracilis* is able to withstand long periods of darkness and sudden light bursts of variable intensity. The capacity to recover safely and rapidly relies on the maintenance, through the dark period, of the main components of the photosynthetic machinery (PSII and pigments, Rubisco).

The flexibility of *C. neogracilis* probably relies on the induction of xanthophyll-related NPQ and possible induction of alternate electron pathways. The extremely low expenditures of energy during darkness - suggested by undetectable organic carbon consumption during one month in darkness- is one extremely important aspect that was not directly studied in this work and needs further investigation.

Compliance with Ethical Standards

The authors declare that they have no conflict of interest.

References

Antia NJ, Cheng JY 1970. The survival of axenic cultures of marine planktonic algae from prolonged exposure to darkness at 20°C. *Phycologia* 9:179-183.

Arrigo KR, Mills MM, Kropuenske LR, van Dijken GL, Alderkamp A-C, Robinson DH 2010. Photophysiology in two major southern ocean phytoplankton taxa: photosynthesis and growth of *Phaeocystis antarctica* and *Fragilariopsis cylindrus* under different irradiance levels. *Integr. Comp. Biol.* 50:950-966.

Bailey S, Melis A, Mackey KRM, Cardol P, Finazzi G, van Dijken G, Berg GM, Arrigo K, Shrager J, Grossman A 2008. Alternative photosynthetic electron flow to oxygen in marine *Synechococcus*. *Biochimica et Biophysica Acta (BBA) - Bioenergetics* 1777:269-276.

Baldisserotto C, Ferroni L, Andreoli C, Fasulo MP, Bonora A, Pancaldi S 2005. Dark-acclimation of the chloroplast in *Koliella antarctica* exposed to a simulated austral night condition. *Arct. Antarct. Alp. Res.* 37:146-156.

Balzano S, Gourvil P, Siano R, Chanoine M, Marie D, Lessard S, Sarno D, Vaulot D 2012. Diversity of cultured photosynthetic flagellates in the northeast Pacific and Arctic Oceans in summer. *Biogeosciences* 9:4553-4571.

Balzano S, Percopo I, Siano R, Gourvil P, Chanoine M, Marie D, Vaulot D, Sarno D 2017. Morphological and genetic diversity of Beaufort Sea diatoms with high contributions from the *Chaetoceros neogracilis* species complex. *J. Phycol.* 53:161-187.

Berge J, Daase M, Renaud Paul E, Ambrose William G, Jr., Darnis G, Last Kim S, Leu E, Cohen Jonathan H, Johnsen G, Moline Mark A, Cottier F, Varpe Ø, Shunatova N, Bałazy P, Morata N, Massabuau J-C, Falk-Petersen S, Kosobokova K, Hoppe Clara JM, Węsławski Jan M, Kukliński P, Legeżyńska J, Nikishina D, Cusa M, Kędra M, Włodarska-Kowalczuk M, Vogedes D, Camus L, Tran D, Michaud E, Gabrielsen Tove M, Granovitch A, Gonchar A, Krapp R, Callesen Trine A 2015. Unexpected Levels of Biological Activity during the Polar Night Offer New Perspectives on a Warming Arctic. *Curr. Biol.* 25:2555-2561.

549
550 Brunet C, Casotti R, Vantrepotte V, Conversano F 2007. Vertical variability and diel dynamics
551 of picophytoplankton in the Strait of Sicily, Mediterranean Sea, in summer. *Mar. Ecol. Prog.*
552 *Ser.* 346:15-26.
553
554 Brunet C, Casotti R, Vantrepotte V, Corato F, Conversano F 2006. Picophytoplankton diversity
555 and photoacclimation in the Strait of Sicily (Mediterranean Sea) in summer. I. Mesoscale
556 variations. *Aquat. Microb. Ecol.* 44:127-141.
557
558 Bunt JS, Lee CC 1972. Data on the Composition and Dark Survival of Four Sea-Ice Microalgae.
559 *Limnol. Oceanogr.* 17:458-461.
560
561 Cardol P, Bailleul B, Rappaport F, Derelle E, Béal D, Breyton C, Bailey S, Wollman FA,
562 Grossman A, Moreau H, Finazzi G 2008. An original adaptation of photosynthesis in the
563 marine green alga *Ostreococcus*. *Proceedings of the National Academy of Sciences* 105:7881-
564 7886.
565
566 Dehning I, Tilzer MM 1989. Survival of *Scenedesmus acuminatus* (chlorophyceae) in darkness.
567 *J. Phycol.* 25:509-515.
568
569 Deventer B, Heckman C 1996. Effects of prolonged darkness on the relative pigment content
570 of cultured diatoms and green algae. *Aquatic Science* 58:241-252.
571
572 Fang X, Sommer U 2017. Overwintering effects on the spring bloom dynamics of
573 phytoplankton. *J. Plankton Res.* 39:772-780.
574
575 Ferroni L, Baldisserotto C, Zennaro V, Soldani C, Fasulo MP, Pancaldi S 2007. Acclimation to
576 darkness in the marine chlorophyte *Koliella antarctica* cultured under low salinity:
577 hypotheses on its origin in the polar environment. *Eur. J. Phycol.* 42:91-104.
578
579 Genty B, Briantais J-M, Baker NR 1989. The relationship between the quantum yield of
580 photosynthetic electron transport and quenching of chlorophyll fluorescence. *Biochimica et*
581 *Biophysica Acta (BBA) - General Subjects* 990:87-92.
582
583 Goss R, Jakob T 2010. Regulation and function of xanthophyll cycle-dependent
584 photoprotection in algae. *Photosynth. Res.* 106:103-122.
585
586 Grossman AR, Mackey KRM, Bailey S 2010. A perpective on photosynthesis in the oligotrophic
587 oceans: hypothesis concerning alternate routes of electron flow. *J. Phycol.* 46:629-634.
588
589 Guillard RRL 1975. Culture of phytoplankton for feeding marine invertebrates. *In* W. L. S. a.
590 M. H. C. (Eds) *Culture of invertabrate animals*, N.Y.:29-66.
591
592 Hancke K, Lund-Hansen LC, Lamare ML, Højlund Pedersen S, King MD, Andersen P, Sorrell
593 BK 2018. Extreme Low Light Requirement for Algae Growth Underneath Sea Ice: A Case Study
594 From Station Nord, NE Greenland. *Journal of Geophysical Research: Oceans* 123:985-1000.

Hendrickson L, Furbank R, Chow W 2004. A simple alternative approach to assessing the fate of absorbed light energy using chlorophyll fluorescence. *Photosynth. Res.* 82:73-81.

Hughes DJ, Campbell DA, Doblin MA, Kromkamp JC, Lawrenz E, Moore CM, Oxborough K, Prášil O, Ralph PJ, Alvarez MF, Suggett DJ 2018a. Roadmaps and Detours: Active Chlorophyll-a Assessments of Primary Productivity Across Marine and Freshwater Systems. *Environ. Sci. Technol.* 52:12039-12054.

Hughes DJ, Varkey D, Doblin MA, Ingleton T, McInnes A, Ralph PJ, van Dongen-Vogels V, Suggett DJ 2018b. Impact of nitrogen availability upon the electron requirement for carbon fixation in Australian coastal phytoplankton communities. *Limnol. Oceanogr.* 63:1891-1910.

Huot Y, Babin M 2010. Overview of Fluorescence Protocols: Theory, Basic Concepts, and Practice. *In* D. J. Suggett, O. Prášil and M. A. Borowitzka *Chlorophyll a Fluorescence in Aquatic Sciences: Methods and Applications*. Springer Netherlands. 4**:**31-74.

Jakob T, Goss R, Wilhelm C 1999. Activation of Diadinoxanthin De-Epoxidase Due to a Chiororespiratory Proton Gradient in the Dark in the Diatom *Phaeodactylum tricornutum*. *Plant Biology* 1:76-82.

Kropuenske LR, Mills MM, van Dijken GL, Alderkamp A-C, Mine Berg G, Robinson DH, Welschmeyer NA, Arrigo KR 2010. Strategies and rates of photoacclimation in two major southern ocean phytoplankton taxa: *Phaeocystis antarctica* (Haptophyta) and *Fragilariopsis cylindrus* (Bacillariophyceae). *J. Phycol.* 46:1138-1151.

Kropuenske LR, Mills MM, Van Dijken GL, Bailey S, Robinson DH, Welschmeyer NA, Arrigo KR 2009. Photophysiology in two major Southern Ocean phytoplankton taxa: Photoprotection in *Phaeocystis antarctica* and *Fragilariopsis cylindrus*. 54:21.

Kvernvik AC, Hoppe CJM, Lawrenz E, Prášil O, Greenacre M, Wiktor JM, Leu E 2018. Fast reactivation of photosynthesis in arctic phytoplankton during the polar night1. *J. Phycol.* 54:461-470.

Lacour T, Larivière J, Babin M 2017. Growth, Chl *a* content, photosynthesis, and elemental composition in polar and temperate microalgae. *Limnol. Oceanogr.* 62:43-58.

Lacour T, Larivière J, Ferland J, Bruyant F, Lavaud J, Babin M 2018. The Role of Sustained Photoprotective Non-photochemical Quenching in Low Temperature and High Light Acclimation in the Bloom-Forming Arctic Diatom *Thalassiosira gravida*. *Frontiers in Marine Science* 5.

Lavaud J, Strzepek RF, Kroth PG 2007. Photoprotection capacity differs among diatoms: Possible consequences on the spatial distribution of diatoms related to fluctuations in the underwater light climate. *Limnol. Oceanogr.* 52:1188-1194.

641 Lavaud J, van Gorkom HJ, Etienne AL 2002. Photosystem II electron transfer cycle and
642 chlororespiration in planktonic diatoms. *Photosynth. Res.* 74:51-59.
643
644 Leu E, Mundy CJ, Assmy P, Campbell K, Gabrielsen TM, Gosselin M, Juul-Pedersen T, Gradinger
645 R 2015. Arctic spring awakening – Steering principles behind the phenology of vernal ice
646 algal blooms. *Prog. Oceanogr.* 139:151-170.
647
648 Lewis MR, Smith JC 1983. A small volume, short-incubation-time method for measure-ment
649 of photosynthesis as a function of incident irradiance. *Mar. Ecol.-Prog. Ser.* 13:99-102.
650
651 Lüder UH, Wiencke C, Knoetzel J 2002. Acclimation of photosynthesis and pigments during
652 and after six months of darkness in *Palmaria decipiens* (rhodophyta): a study to simulate
653 antarctic winter sea ice cover. *J. Phycol.* 38:904-913.
654
655 Lundholm N, Ribeiro S, Andersen TJ, Koch T, Godhe A, Ekelund F, Ellegaard M 2011. Buried
656 alive – germination of up to a century-old marine protist resting stages. *Phycologia* 50:629-
657 640.
658
659 MacIntyre HL, Cullen JJ 2005. Using cultures to investigate the physiological ecology of
660 microalgae. *In* R. A. Anderson *Algal Culturing Techniques*. Academic Press**:**287-326
661
662 MacIntyre HL, Sharkey TD, Geider RJ 1997. Activation and deactivation of ribulose-1,5-
663 bisphosphate carboxylase/oxygenase (Rubisco) in three marine microalgae. *Photosynth. Res.*
664 51:93-106.
665
666 Mackey KRM, Paytan A, Grossman AR, Bailey S 2008. A photosynthetic strategy for coping in
667 a high-light, low-nutrient environment. *Limnol. Oceanogr.* 53:14.
668
669 Martin A, McMinn A, Heath M, Hegseth EN, Ryan KG 2012. The physiological response to
670 increased temperature in over-wintering sea ice algae and phytoplankton in McMurdo
671 Sound, Antarctica and Tromso Sound, Norway. *J. Exp. Mar. Biol. Ecol.* 428:57-66.
672
673 Maxwell K, Johnson GN 2000. Chlorophyll fluorescence—a practical guide. *J. Exp. Bot.* 51:659-
674 668.
675
676 McMinn A, Ashworth C, Ryan K 1999. Growth and productivity of Antarctic sea ice algae
677 under PAR and UV irradiances. *Bot. Mar.* 42:401-407.
678
679 McMinn A, Martin A 2013. Dark survival in a warming world. *Proceedings of the Royal Society*
680 *B: Biological Sciences* 280:20122909.
681
682 Mills MM, Kropuenske LR, van Dijken GL, Alderkamp A-C, Berg GM, Robinson DH,
683 Welschmeyer NA, Arrigo KR 2010. Photophysiology in two southern ocean phytoplankton
684 taxa: photosynthesis of *Phaeocystis antarctica* (Prymnesiophyceae) and *Fragilariopsis*
685 *cylindrus* (Bacillariophyceae) under simulated mixed-layer irradiance. *J. Phycol.* 46:1114-
686 1127.

Morgan-Kiss RM, Priscu JC, Pocock T, Gudynaite-Savitch L, Huner NPA 2006. Adaptation and Acclimation of Photosynthetic Microorganisms to Permanently Cold Environments. *Microbiol. Mol. Biol. Rev.* 70:222-252.

Mundy CJ, Gosselin M, Ehn J, Gratton Y, Rossnagel A, Barber DG, Martin J, Tremblay J-É, Palmer M, Arrigo KR, Darnis G, Fortier L, Else B, Papakyriakou T 2009. Contribution of under-ice primary production to an ice-edge upwelling phytoplankton bloom in the Canadian Beaufort Sea. *Geophysical Research Letters* 36:L17601.

Murphy AM, Cowles TJ 1997. Effects of darkness on multi-excitation in vivo fluorescence and survival in a marine diatom. *Limnol. Oceanogr.* 42:1444-1453.

Murphy CD, Ni G, Li G, Barnett A, Xu K, Grant-Burt J, Liefer JD, Suggett DJ, Campbell DA 2016. Quantitating active photosystem II reaction center content from fluorescence induction transients. *Limnology and Oceanography: Methods* 15:54-69.

Murphy CD, Roodvoets MS, Austen EJ, Dolan A, Barnett A, Campbell DA 2017. Photoinactivation of Photosystem II in *Prochlorococcus* and *Synechococcus*. *PLoS ONE* 12:e0168991.

Nymark M, Valle KC, Hancke K, Winge P, Andresen K, Johnsen G, Bones AM, Brembu T 2013. Molecular and Photosynthetic Responses to Prolonged Darkness and Subsequent Acclimation to Re-Illumination in the Diatom *Phaeodactylum tricornutum*. *PLoS ONE* 8:e58722.

Oguchi R, Terashima I, Kou J, Chow WS 2011. Operation of dual mechanisms that both lead to photoinactivation of Photosystem II in leaves by visible light. *Physiol. Plant* 142:47-55.

Oxborough K, Moore CM, Suggett DJ, Lawson T, Chan HG, Geider RJ 2012. Direct estimation of functional PSII reaction center concentration and PSII electron flux on a volume basis: a new approach to the analysis of Fast Repetition Rate fluorometry (FRRf) data. *Limnology and Oceanography: Methods* 10:142-154.

Palmisano AC, Sullivan CW 1982. Physiology of sea ice diatoms. I. response of three polar diatoms to a simulated summer-winter transition. *J. Phycol.* 18:489-498.

Palmisano AC, Sullivan CW 1983. Physiology of sea ice diatoms. II. Dark survival of three polar diatoms. *Can. J. Microbiol.* 29:157-160.

Parsons TR, Maita Y, Lalli CM 1984. 5.1 - Photosynthesis as Measured by the Uptake of Radioactive Carbon. *In* T. R. P. M. M. Lalli *A Manual of Chemical & Biological Methods for Seawater Analysis*. Pergamon, Amsterdam**:**115-120.

Peters E 1996. Prolonged darkness and diatom mortality .2. Marine temperate species. *J. Exp. Mar. Biol. Ecol.* 207:43-58.

Peters E, Thomas DN 1996. Prolonged darkness and diatom mortality I: Marine Antarctic species. *J. Exp. Mar. Biol. Ecol.* 207:25-41.

Petrou K, Doblin M, Ralph P 2011. Heterogeneity in the photoprotective capacity of three Antarctic diatoms during short-term changes in salinity and temperature. *Mar. Biol.* 158:1029-1041.

Petrou K, Hill R, Brown CM, Campbell DA, Doblin MA, Ralph PJ 2010. Rapid photoprotection in sea-ice diatoms from the East Antarctic pack ice. *Limnol. Oceanogr.* 55:8.

Petrou K, Kranz SA, Trimborn S, Hassler CS, Ameijeiras SB, Sackett O, Ralph PJ, Davidson AT 2016. Southern Ocean phytoplankton physiology in a changing climate. *J. Plant Physiol.* 203:135-150.

Petrou K, Ralph P 2011. Photosynthesis and net primary productivity in three Antarctic diatoms: possible significance for their distribution in the Antarctic marine ecosystem. *Mar. Ecol. Prog. Ser.* 437:27-40.

Platt T, Gallegos CL, Harrison WG 1980. Photoinhibition of photosynthesis in natural assemblages of marine phytoplankton. *J. Mar. Res.* 38:687-701.

Popels LC, Hutchins DA 2002. Factors affecting dark survival of the brown tide alga *Aureococcus anophagefferens* (Pelagophyceae). *J. Phycol.* 38:738-744.

Poulin M, Daugbjerg N, Gradinger R, Ilyash L, Ratkova T, von Quillfeldt C 2011. The pan-Arctic biodiversity of marine pelagic and sea-ice unicellular eukaryotes: a first-attempt assessment. *Mar. Biod.* 41:13-28.

Reeves S, McMinn A, Martin A 2011. The effect of prolonged darkness on the growth, recovery and survival of Antarctic sea ice diatoms. *Polar Biol.* 34:1019-1032.

Rivkin RB, Putt M 1987. Heterotrophy and photoheterotrophy by antarctic microalgae - light-dependent incorporation of amino-acids and glucose. *J. Phycol.* 23:442-452.

Sakshaug E 2004. Primary and secondary production in Arctic seas. *In* E. R. Stein and R.W.Macdonald *The Organic Carbon Cycle in the Arctic Ocean*. Springer, Berlin**:**57-81.

Schaub I, Wagner H, Graeve M, Karsten U 2017. Effects of prolonged darkness and temperature on the lipid metabolism in the benthic diatom *Navicula perminuta* from the Arctic Adventfjorden, Svalbard. *Polar Biol.* 40:1425-1439.

Schuback N, Hoppe CJM, Tremblay J-É, Maldonado MT, Tortell PD 2017. Primary productivity and the coupling of photosynthetic electron transport and carbon fixation in the Arctic Ocean. *Limnol. Oceanogr.* 62:898-921.

779 Schuback N, Schallenberg C, Duckham C, Maldonado MT, Tortell PD 2015. Interacting Effects
780 of Light and Iron Availability on the Coupling of Photosynthetic Electron Transport and CO2-
781 Assimilation in Marine Phytoplankton. *PLoS ONE* 10:e0133235.
782
783 Silsbe GM, Oxborough K, Suggett DJ, Forster RM, Ihnken S, Komárek O, Lawrenz E, Prášil O,
784 Röttgers R, Šicner M, Simis SGH, Van Dijk MA, Kromkamp JC 2015. Toward autonomous
785 measurements of photosynthetic electron transport rates: An evaluation of active
786 fluorescence-based measurements of photochemistry. *Limnology and Oceanography:*
787 *Methods* 13:138-155.
788
789 Smayda TJ, Mitchell-Innes B 1974. Dark survival of autotrophic, planktonic marine diatoms.
790 *Mar. Biol.* 25:195-202.
791
792 Smith AE, Morris I 1980. Pathways of carbon assimilation in phytoplankton from the
793 antarctic ocean. *Limnol. Oceanogr.* 25:865-872.
794
795 Suggett D, Moore CM, Geider R 2010. Estimating Aquatic Productivity from Active
796 Fluorescence Measurements. *In* D. J. Suggett, O. Prášil and M. A. Borowitzka *Chlorophyll a*
797 *Fluorescence in Aquatic Sciences: Methods and Applications*. Springer Netherlands. 4**:**103-127.
798
799 Thomas SL, Campbell DA 2013. Photophysiology of *Bolidomonas pacifica*. *J. Plankton Res.*
800 35:260-269.
801
802 van de Poll WHV, Lagunas M, de Vries T, Visser RJW, Buma AGJ 2011. Non-photochemical
803 quenching of chlorophyll fluorescence and xanthophyll cycle responses after excess PAR and
804 UVR in *Chaetoceros brevis*, *Phaeocystis antarctica* and coastal Antarctic phytoplankton. *Mar.*
805 *Ecol.-Prog. Ser.* 426:119-131.
806
807 Wagner H, Jakob T, Wilhelm C 2006. Balancing the energy flow from captured light to biomass
808 under fluctuating light conditions. *New Phytol.* 169:95-108.
809
810 White AW 1974. Growth of two facultatively heterotrophic marine centric diatoms. *J. Phycol.*
811 10:292-300.
812
813 Wu Y, Jeans J, Suggett D, Finkel Z, Campbell DA 2014. Large centric diatoms allocate more
814 cellular nitrogen to photosynthesis to counter slower RUBISCO turnover rates. *Frontiers in*
815 *Marine Science* 1:1-11.
816
817 Wulff A, Roleda MY, Zacher K, Wiencke C 2008. Exposure to sudden light burst after
818 prolonged darkness - a case study on benthic diatoms in antarctica. *Diatom. Res.* 23:519-532.
819
820 Young JN, Goldman JAL, Kranz SA, Tortell PD, Morel FMM 2015. Slow carboxylation of
821 Rubisco constrains the rate of carbon fixation during Antarctic phytoplankton blooms. *New*
822 *Phytol.* 205:172–181.
823

824 Zapata M, Rodriguez F, Garrido JL 2000. Separation of chlorophylls and carotenoids from
825 marine phytoplankton: a new HPLC method using a reversed phase C8 column and pyridine-
826 containing mobile phases. *Mar. Ecol. Prog. Ser.* 195:29-45.
827
828 Zhu Y, Ishizaka J, Tripathy SC, Wang S, Sukigara C, Goes J, Matsuno T, Suggett DJ 2017.
829 Relationship between light, community composition and the electron requirement for carbon
830 fixation in natural phytoplankton. *Mar. Ecol. Prog. Ser.* 580:83-100.
831
832

Figure1_Lacour *et al.*

Figure 1: Changes in cell density of *Chaetoceros neogracilis* cultures exposed to 4 different light cycles after 1 month in total darkness at 0°C (A). Mean growth rates of triplicate cultures computed between days 1 and 6 are indicated on the graph. Note that mean growth rates were equal in cells exposed to 41 and 154 µmol photon m^{-2} s^{-1}. Each data point is the mean ± SD of the 3 different cultures. Instantaneous growth rates of *C. neogracilis* measured during the first eight hours, between eight and 32 hours and between 32 and 54 hours under different light cycles after 1 month in darkness (B). Each bar is the mean ± SD of the 3 different cultures.

Figure2_Lacour *et al.*

Figure 2: Changes in photochemical properties of *Chaetoceros neogracilis* at 4 different light cycles after 1 month in total darkness at 0°C. ETR_m (A), E_K^{ETR} (B), α^{ETR} (C) as a function of time under different light cycles. In A, B, C each data point is the mean ± SD of triplicate cultures. Relationship between mean growth irradiance and mean ETR_m, E_K^{ETR} and α^{ETR} (D). In D, each data point is the mean ± SD of 3 consecutive days (day 3, 4 and 5) from triplicate cultures.

Figure3_Lacour *et al.*

Figure 3: Enlargement of part of Figure 2. ETR_m (A), E_K^{ETR} (B), α^{ETR} (C) as a function of time under different light cycles. In A, B, C each data point is the mean ± SD of triplicate cultures.

Figure4_Lacour *et al.*

Figure 4: Biochemical characteristics of cells acclimated to 23 µmol photon m^{-2} s^{-1} or to the dark. Cell diameter (A), C\N (B), Chl *a*/C (C), (Dd + Dt)/Chl *a*, DES (DES =Dt/(Dd+Dt)), Dt/Chl *a* and β-carotene/Chl *a* (D), Rubisco to carbon ratio and apparent Rubisco catalytic turnover rate (s^{-1})(E) in cultures acclimated to 23 µmol photon m^{-2} s^{-1} (white bars) and after 1 month in the dark (black bars). Each bar is the mean of 3 different cultures. Error bars represent standard deviations. Asterisks indicate significant differences (one asterisk : $P<0.05$, two: $P<0.001$) between light and dark acclimated cells.

865

866 **Figure5_Lacour *et al.***

867

868 **Figure 5:** Estimated fraction of absorbed irradiance consumed via photochemistry (Φ_{PSII}),
869 regulated thermal dissipation (Φ_{NPQ}) and non-regulated thermal dissipation and fluorescence ($\Phi_{f,D}$)
870 as a function of incubation irradiance for cultures of *Chaetoceros neogracilis* acclimated to 23
871 µmol photon m^{-2} s^{-1} (A) and incubated one month in the dark (B). Those parameters were defined
872 by Hendrickson et al. (2004) to compare the fate of absorbed light. Each point is the mean of 3
873 different cultures. Error bars represent standard deviations.

874

875 **Figure6_Lacour *et al.***

876

877 **Figure 6:** PSII activity in the light and in the dark. F_v/F_m, σ_{PSII} and proxy for PSII content F_O/
878 (σ_{PSII} Chl *a*) (A), ETR_m and E_K^{ETR} (B), α^{ETR} (C) in cultures acclimated to 23 µmol photon m^{-2} s^{-1}
879 (white bars) and after 1 month in the dark (black bars). Each bar is the mean of 3 different cultures.
880 Error bars represent standard deviations. Asterisks indicate significant differences (one asterisk :
881 $P<0.05$, two: $P<0.001$) between light and dark acclimated cells.

882

883 **Figure7_Lacour *et al.***

884

885 **Figure 7:** Carbon specific fixation rate versus incubation irradiance curves of cells incubated in
886 the dark for one month or acclimated to 10, 50 and 80 µmol photon m^{-2} s^{-1} (minimum of 10
887 generations, see methods) (A). Each data point is the mean of measures from 3 different cultures.
888 Error bars represent standard deviations. α^* (B) and P^C_m (C) of cell incubated in the dark (black
889 bars, mean ± SD of triplicate cultures incubated 1 month in the dark) or pooled determinations for
890 cultures acclimated to light (white bars, mean ± SD of pooled determinations from 10, 50 and 80
891 µmol photon m^{-2} s^{-1}). Asterisks indicate significant differences (one asterisk: $P<0.05$, two:
892 $P<0.001$) between light and dark acclimated cells.

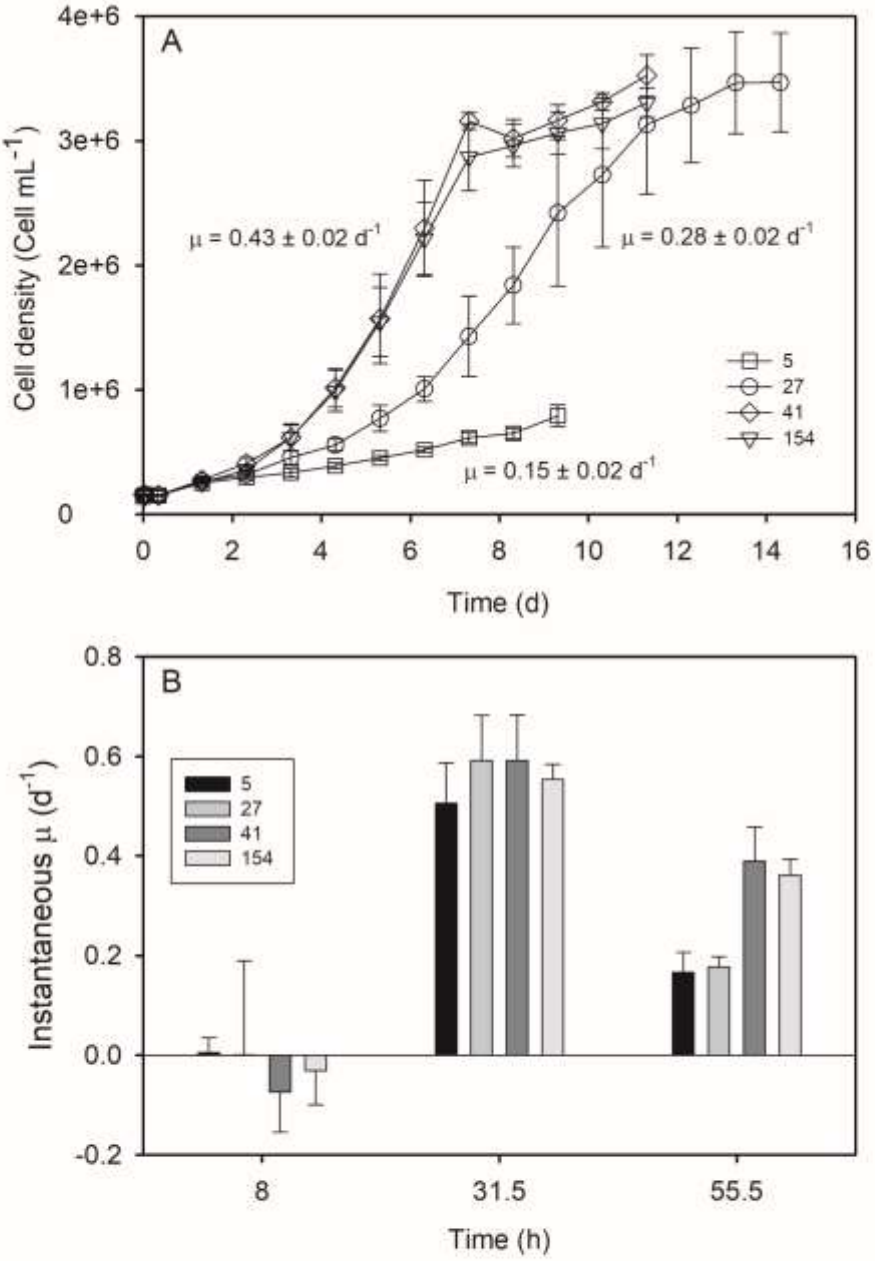
A
Cell density (Cell mL^{-1})
Time (d)
μ = 0.43 ± 0.02 d^{-1}
μ = 0.28 ± 0.02 d^{-1}
μ = 0.15 ± 0.02 d^{-1}
5
27
41
154
B
Instantaneous μ (d^{-1})
Time (h)
8
31.5
55.5

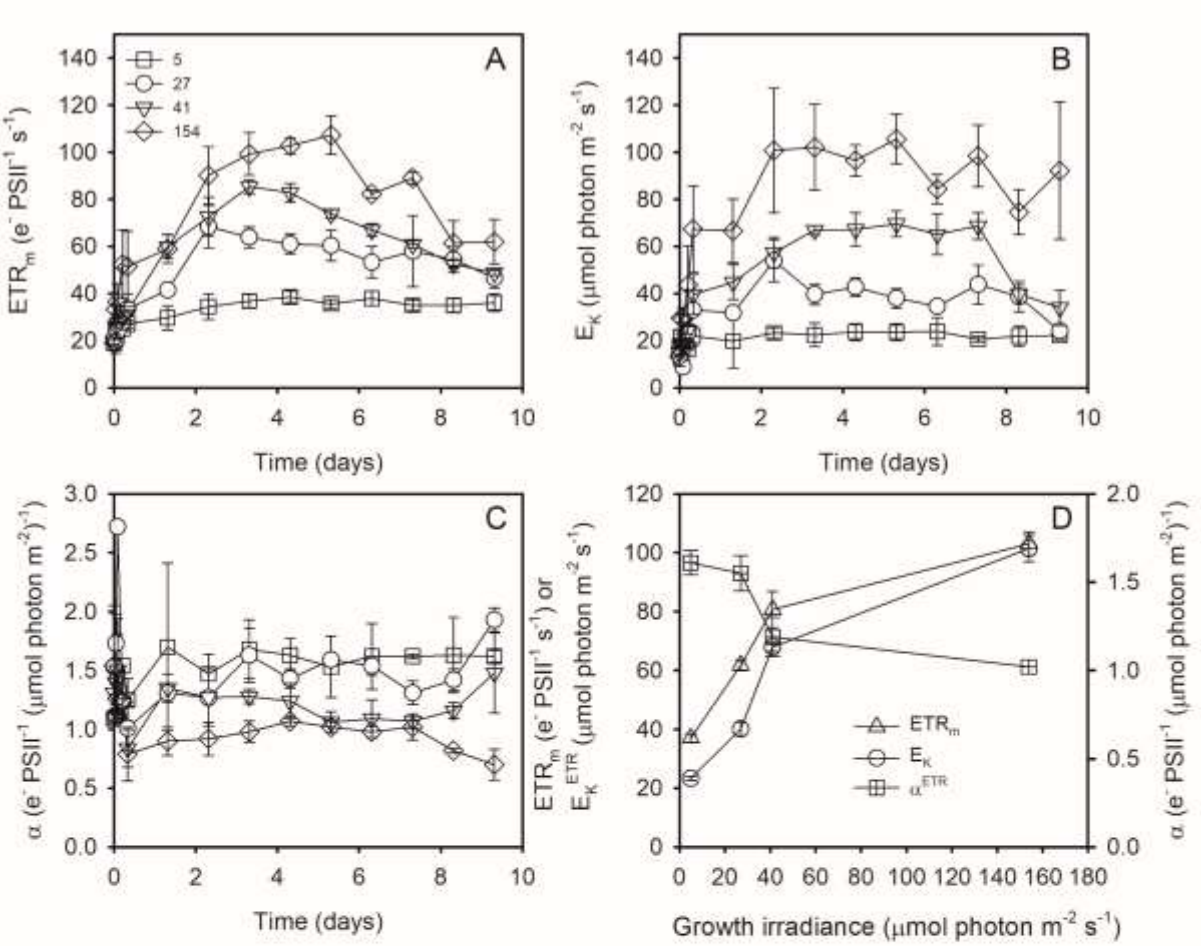
A
B
C
D
5
27
41
154
ETR$_m$ (e$^-$ PSII^{-1} s^{-1})
E$_K$ (µmol photon m^{-2} s^{-1})
α (e$^-$ PSII^{-1} (µmol photon m^{-2})$^{-1}$)
ETR$_m$ (e$^-$ PSII^{-1} s^{-1}) or
E$_K^{ETR}$ (µmol photon m^{-2} s^{-1})
Time (days)
Growth irradiance (µmol photon m^{-2} s^{-1})
ETR$_m$
E$_K$
α^{ETR}

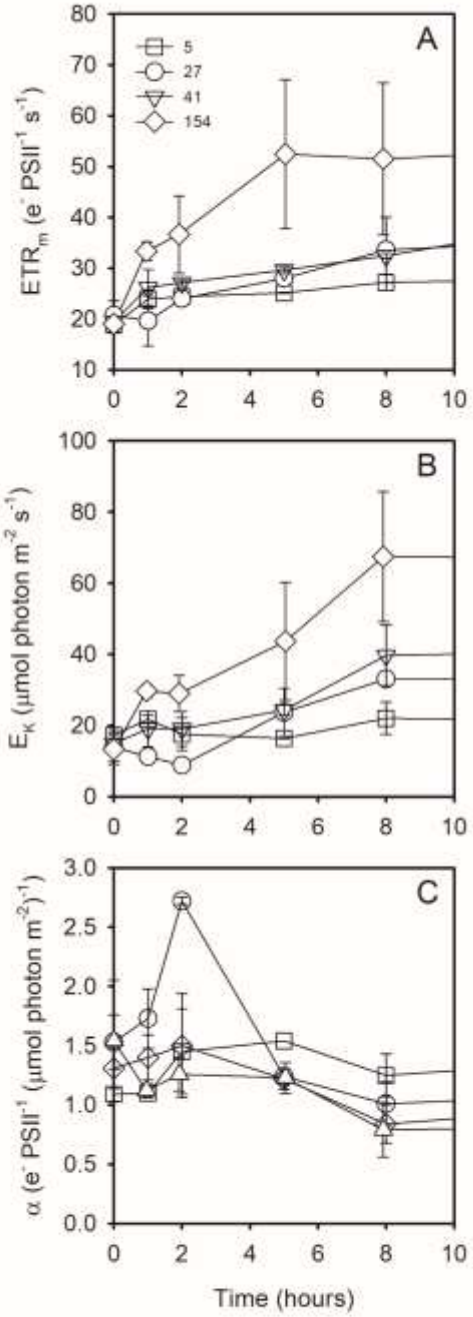
A
B
C
5
27
41
154
ETR$_m$ (e$^-$ PSII^{-1} s^{-1})
E_K (µmol photon m^{-2} s^{-1})
α (e$^-$ PSII^{-1} (µmol photon m^{-2})$^{-1}$)
Time (hours)

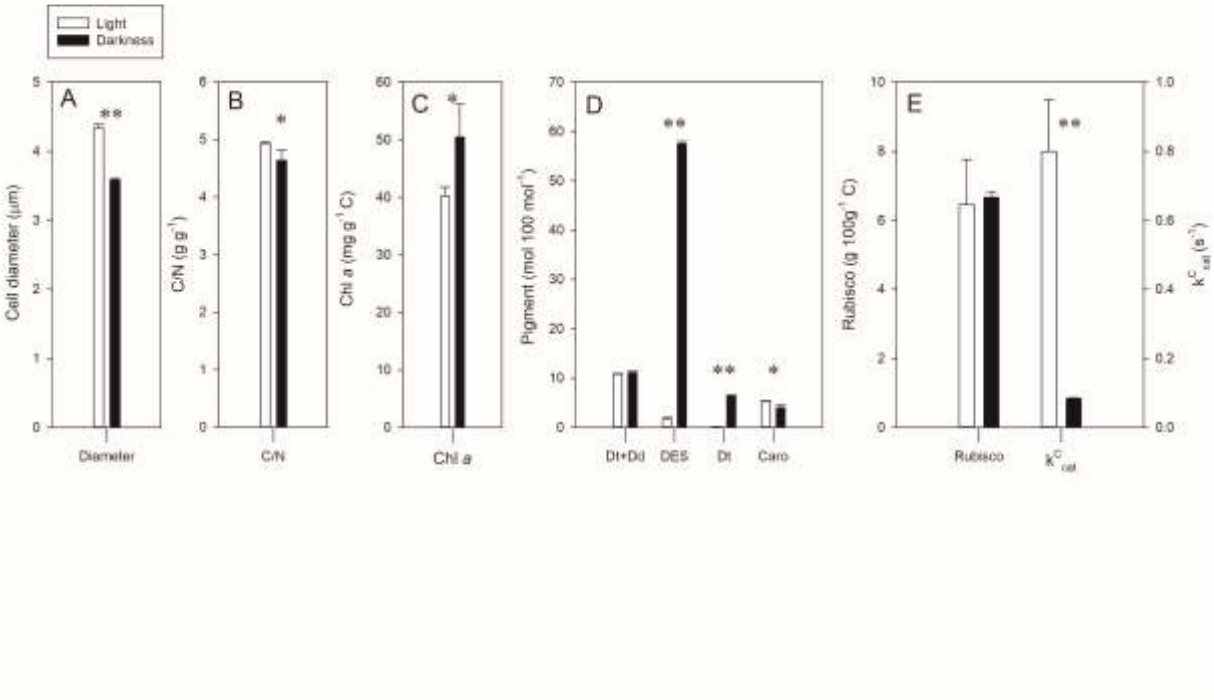
Light
Darkness
A
B
C
D
E
Cell diameter (µm)
C/N (g g⁻¹)
Chl a (mg g⁻¹ C)
Pigment (mol 100 mol⁻¹)
Rubisco (g 100g⁻¹ C)
Diameter
C/N
Chl a
Dt+Dd
DES
Dt
Caro
Rubisco

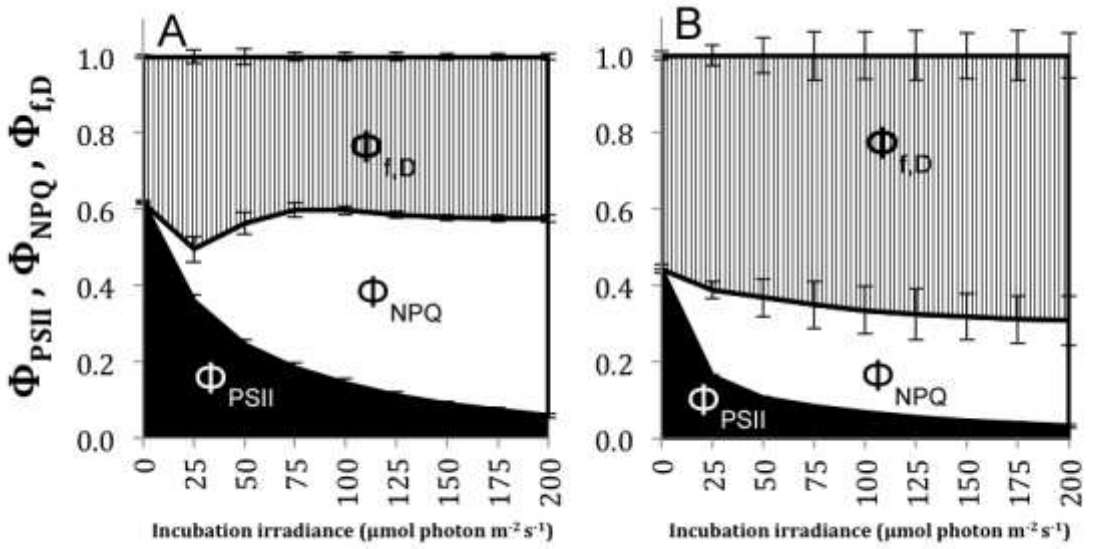
A
B
Φ f,D
Φ NPQ
Φ PSII
Φ PSII , Φ NPQ , Φ f,D
Incubation irradiance (µmol photon m⁻² s⁻¹)

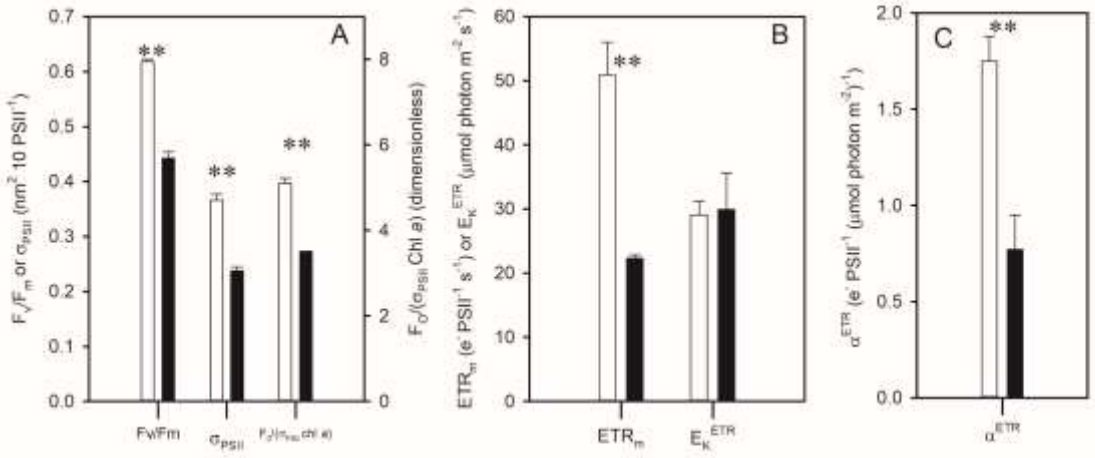
A
B
C
**
Fv/Fm
σ_{PSII}
$F_O/(\sigma_{PSII}$ Chl a)
ETR_m
E_K^{ETR}
α^{ETR}
F_v/F_m or σ_{PSII} (nm^2 10 PSII^{-1})
$F_O/(\sigma_{PSII}$ Chl a) (dimensionless)
ETR_m (e$^-$ PSII^{-1} s^{-1}) or E_K^{ETR} (µmol photon m^{-2} s^{-1})
α^{ETR} (e$^-$ PSII^{-1} (µmol photon m^{-2})$^{-1}$)

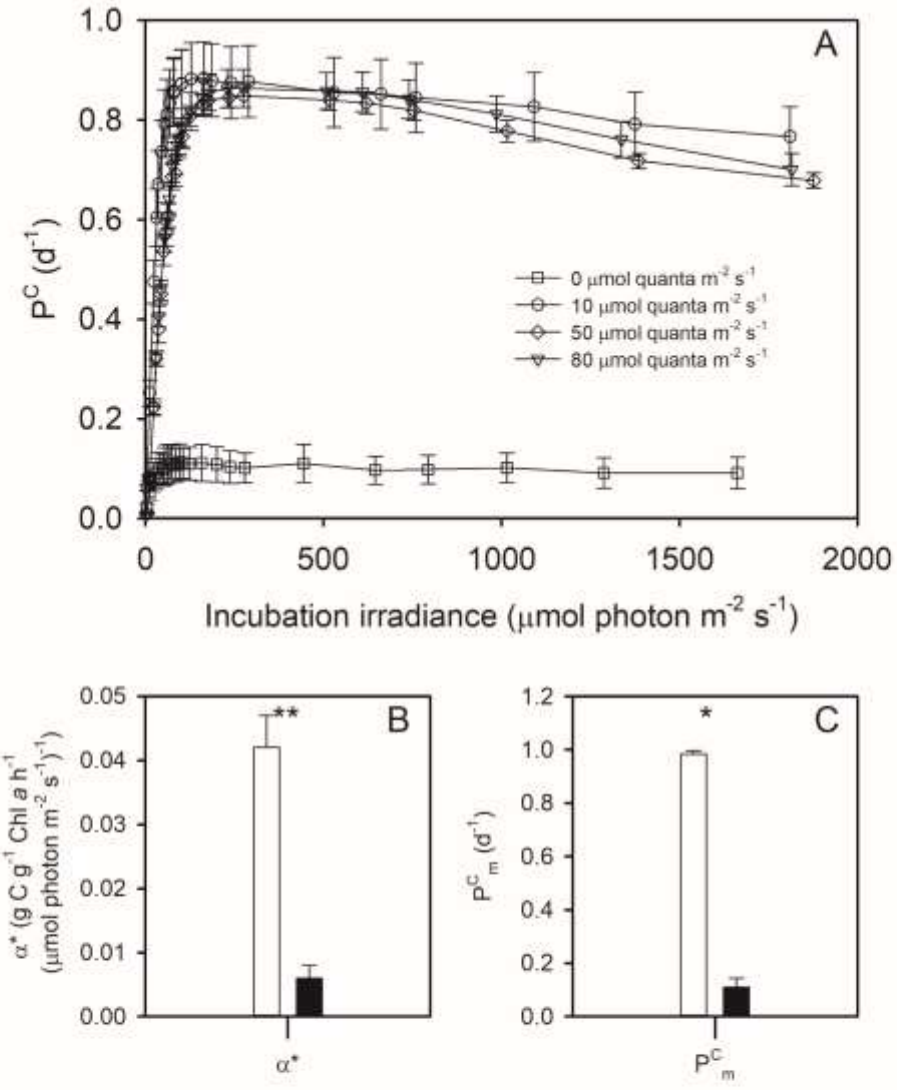
A
1.0
0.8
0.6
0.4
0.2
0.0
P^C (d^{-1})
0 μmol quanta m^{-2} s^{-1}
10 μmol quanta m^{-2} s^{-1}
50 μmol quanta m^{-2} s^{-1}
80 μmol quanta m^{-2} s^{-1}
0
500
1000
1500
2000
Incubation irradiance (μmol photon m^{-2} s^{-1})

B
**
0.05
0.04
0.03
0.02
0.01
0.00
α* (g C g^{-1} Chl *a* h^{-1} (μmol photon m^{-2} s^{-1})$^{-1}$)
α*

C
*
1.2
1.0
0.8
0.6
0.4
0.2
0.0
P^C_m (d^{-1})
P^C_m

Online resources

Decoupling light harvesting, electron transport and carbon fixation during prolonged darkness supports rapid recovery upon re-illumination in the polar diatom *Chaetoceros neogracilis*

Thomas Lacour [1,2*] Corresponding author, Thomas.Lacour@*ifremer*.fr , Philippe-Israël Morin [1], Théo Sciandra [1], Natalie Donaher [3], Douglas A. Campbell [3] , Joannie Ferland [1], Marcel Babin [1]

1- Takuvik Joint International Laboratory, CNRS (France) & ULaval (Canada), Pavillon Alexandre-Vachon, Local 2078, 1045, avenue de la Médecine, Département de Biologie, Université Laval, Québec, QC G1V 0A6, Canada
2- IFREMER, Physiol & Biotechnol Algae Labs, Rue Ile Yeu, F-44311 Nantes, France
3- Department of Biology, Mount Allison University, Sackville NB, Canada E4L1G7

* Present address: Ifremer, PBA, Rue de l'Ile d'Yeu, BP21105, 44311 Nantes Cedex 03, France
Tel: 0033 (0)2 40 37 41 09

Online resource 1: Diel light cycle applied during light recovery. Irradiance as a function of the time of the day in cultures previously incubated in the dark for 1 month. Triplicate cultures were illumined at each light cycle. Mean diel growth irradiances were 154, 41, 27 and 5 µmol photon m^{-2} s^{-1}. Maximum growth irradiances (at noon) were 531, 141, 93 and 17 µmol photon m^{-2} s^{-1}.

Online resource 2: Chlorophyll *a* specific absorption coefficient (a* in m^2 mg Chl*a*$^{-1}$) *versus* the wavelength of light in cultures acclimated to 23 µmol photon m^{-2} s^{-1} and after 1 month in the dark (A). Relative difference (in %) between a* at 23 µmol photon m^{-2} s^{-1} and after 1 month in the dark (B).

Online resource 3: σ^{OPT}_{PSII} in cells acclimated to 23 µmol photon m^{-2} s^{-1} (white bars) and after 1 month in the dark (black bars).

Online resource 4: Electron transport rate versus incubation irradiance curves of cells incubated in the dark for one month or acclimated to 23 µmol photon m^{-2} s^{-1}. Each data point is the mean of measures from 3 different cultures. Error bars represent standard deviations. A model (Platt *et al.*, 1980) was fitted to the data to estimate ETR_m, E_K^{ETR}, α^{ETR} and β^{ETR} (see Figure 3, 7 and methods).

Online resource 5: Results of the t-tests comparing photo-physiological parameter at different irradiance of cells acclimated to light and (see statistic section and Figure 4).

Online_resource_1_Lacour *et al.*

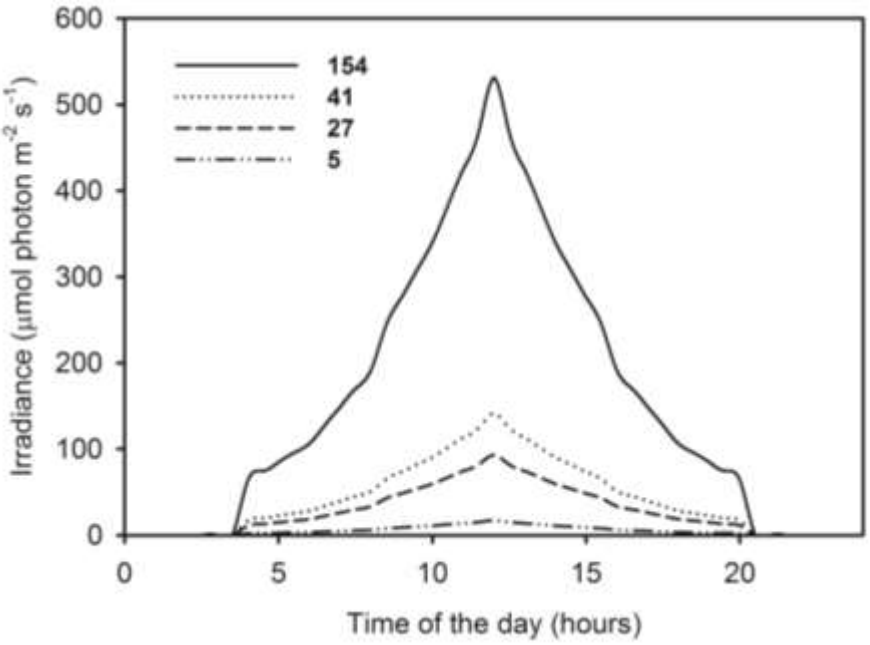

Online resource 1: Diel light cycle applied during light recovery. Irradiance as a function of the time of the day in cultures previously incubated in the dark for 1 month. Triplicate cultures were illumined at each light cycle. Mean diel growth irradiances were 154, 41, 27 and 5 µmol photon m^{-2} s^{-1}. Maximum growth irradiances (at noon) were 531, 141, 93 and 17 µmol photon m^{-2} s^{-1}.

Online_resource_2_Lacour *et al.*

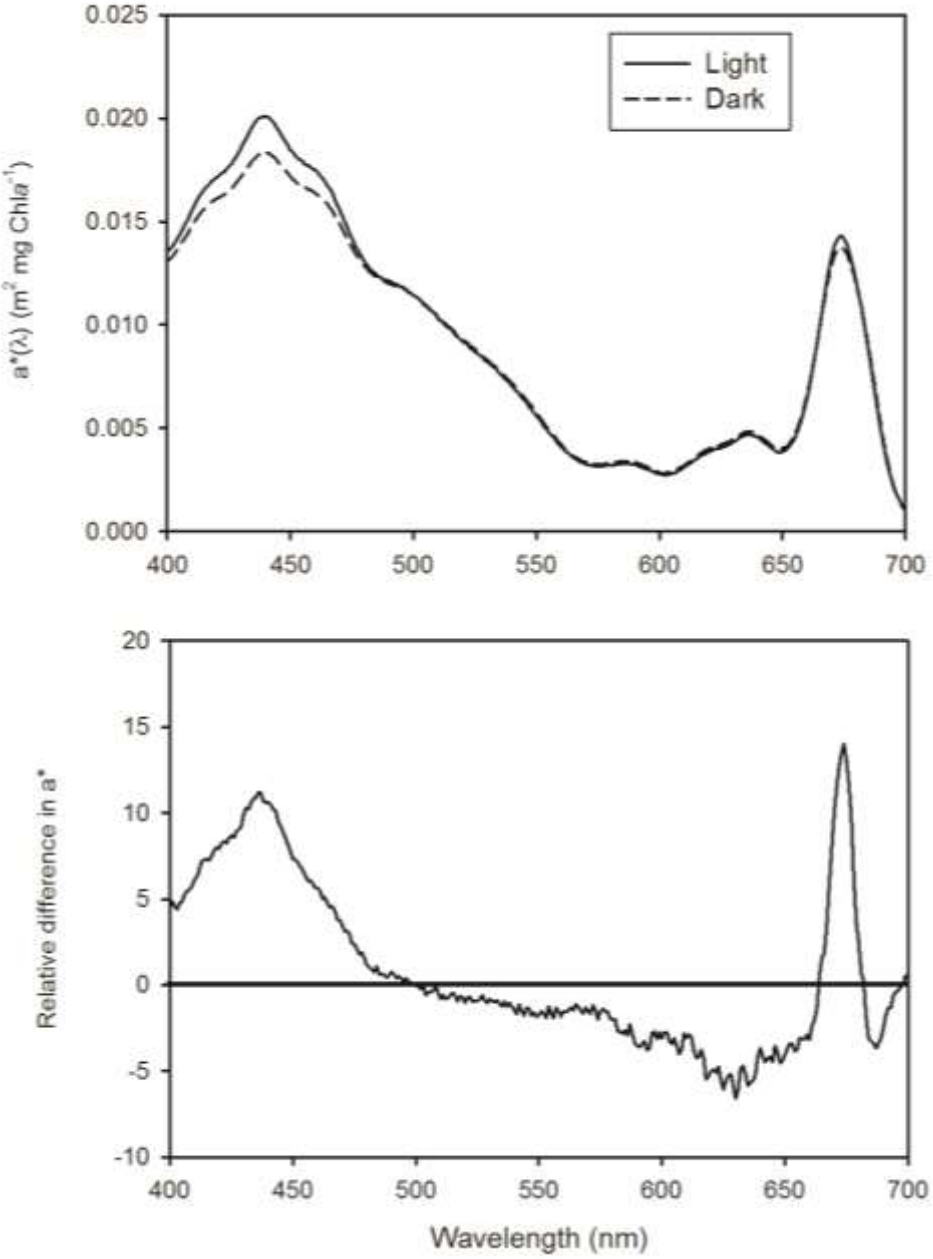

Online resource 2: Chlorophyll *a* specific absorption coefficient (a* in m^2 mg Chla^{-1}) *versus* the wavelength of light in cultures acclimated to 23 µmol photon m^{-2} s^{-1} and after 1 month in the dark (A). Relative difference (in %) between a* at 23 µmol photon m^{-2} s^{-1} and after 1 month in the dark (B).

Online_resource_3_Lacour *et al.*

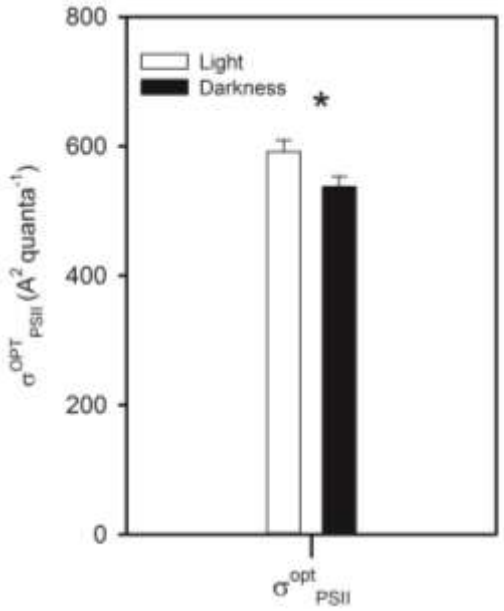

Online resource 3: σ^{OPT}_{PSII} in cells acclimated to 23 µmol photon m^{-2} s^{-1} (white bars) and after 1 month in the dark (black bars).

Online_resource_4_Lacour *et al.*

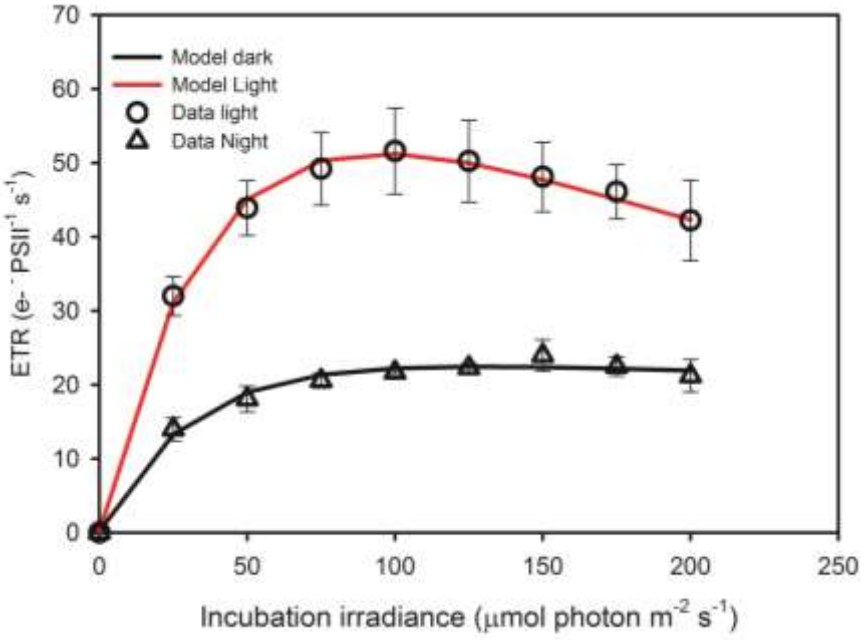

Online resource 4: Electron transport rate versus incubation irradiance curves of cells incubated in the dark for one month or acclimated to 23 µmol photon m^{-2} s^{-1}. Each data point is the mean of measures from 3 different cultures. Error bars represent standard deviations. A model (Platt *et al.*, 1980) was fitted to the data to estimate ETR_m, E_K^{ETR}, α^{ETR} and β^{ETR} (see Figure 3, 7 and methods).

Online_resource_5_Lacour *et al.*

Results of the t-tests comparing photo-physiological parameter at different irradiance of cells acclimated to light and (see statistic section and Figure 5). Results of each test (df, t, p) at each incubation irradiance are presented.

	Φ_{PSII}			Φ_{NPQ}			$\Phi_{f,d}$		
E	df	t	p	df	t	p	df	t	p
0	9	34.55	<0.0001	NA	NA	NA	9	-34.550	<0.0001
25	9	14.678	<0.0001	9	-3.505	0.0067	9	-7.096	<0.0001
50	9	15.869	<0.0001	9	2.139	0.0611	9	-10.084	<0.0001
75	9	11.148	<0.0001	9	7.132	<0.0001	9	-13.592	<0.0001
100	9	9.259	<0.0001	9	10.201	<0.0001	9	-14.832	<0.0001
125	9	9.165	<0.0001	9	11.112	<0.0001	9	-14.174	<0.0001
150	9	9.254	<0.0001	9	13.057	<0.0001	9	-15.326	<0.0001
175	9	9.665	<0.0001	9	13.313	<0.0001	9	-14.734	<0.0001
200	9	5.379	0.0004	9	13.361	<0.0001	9	-16.100	<0.0001

Platt T, Gallegos CL, and Harrison WG. **1980**. Photoinhibition of photosynthesis in natural assemblages of marine phytoplankton. *Journal of Marine Research*. 38:687-701.